JOURNAL OF PROPULSION AND POWER
Vol. 27, No. 4, July–August 2011

Technical Notes

Passing Through the Wind Turbine Thrust Singularity

M. J. Werle*
FloDesign Wind Turbine, Inc.,
Wilbraham, Massachusetts 01095

DOI: 10.2514/1.43909

Nomenclature

A	=	flow cross-sectional area
a	=	induction factor, 1-u_p
C_D	=	disk loss coefficient
C_P	=	power coefficient
C_T	=	thrust coefficient
p	=	pressure
U	=	nondimensional velocity for u near zero
u	=	nondimensional axial velocity
V	=	axial velocity
α	=	flow-domain area ratio
ρ	=	fluid density

Subscripts

a	=	ambient freestream conditions
c	=	properties outside the rotor/disk wake at downstream outlet area
o	=	properties in the rotor/disk wake at downstream outlet area
p	=	conditions at the rotor/disk plane
1,2	=	properties fore and aft of the rotor/disk

I. Introduction

IT HAS long been known that the popular and useful control-volume actuator-disk model for wind turbines encounters a troublesome behavior as the thrust coefficient for the rotor/disk approaches 1, which occurs when the velocity at the rotor/disk approaches half that of the freestream level and the axial velocity at the downstream outlet approaches zero. This is discussed in detail in nearly all texts and papers involving wind turbines (as, for example, in [1–8]). Beyond a thrust-coefficient value of 1, it is well understood that the current version of the model does not apply, because it predicts flow entering the control volume at the downstream outlet, thus negating its further use and leaving a gap in the theory for an important range of the controlling parameters. To date, this gap has been addressed largely with either empirical expressions and/or computational fluid dynamics (CFD) methods. Based on Glauert's 1926 analysis of data taken for windmilling helicopter blades in open-jet wind tunnels (as discussed in [1]) and its adaption to wind turbines by Stoddard [5], it is now widely accepted that the classical model begins to break down somewhere near a rotor/disk velocity ratio of 0.6 (induction factor of 0.4). For larger induction factors, it is assumed that a turbulent-wake state ensues, with reverse and/or unsteady flow effects dominating the flow as the rotor/disk velocity further reduces to zero: i.e., the rotor/disk stalls. It is further widely accepted that Glauert's empirical expression for the rotor/disk performance prevails in this turbulent-wake region, with several attempts at improving its utility, as summarized by Buhl [8]. Additionally, recent CFD studies by Sørensen et al. [6] and Mikkelsen [7] appear to reinforce this empirical model.

Recently, however, two studies [9,10] using control-volume actuator-disk modeling of wind-tunnel blockage influences on rotor/disk performance uncovered an entirely new family of well-behaved steady-state solutions that exist in the turbulent-wake parameter space: i.e., for induction factors from 0.4 all the way to 1. Moreover, the results of [9] implied the existence of a new well-behaved solution family for induction factors above 0.5, even for the zero-blockage condition. The current work provides this new exact solution for induction factors from 0.5 to 1 based on a limit-analysis solution of the control-volume actuator-disk equations. This new solution provides the heretofore missing piece of the basic theory, filling the gap for induction factors of 0.5 to 1. Comparisons of the new analytical solutions with experiments and CFD studies of actuator disks provide strong evidence of its validity. The relevance of the results to CFD modeling, wind-tunnel testing, and/or field testing of wind turbines is discussed.

II. Analysis and Results

The analysis follows that provided in [9]. It begins by employing the control volume shown in Fig. 1 and considers the limit as the domain cross-sectional area A_c becomes infinitely large compared with the rotor/disk area A_p. The governing equations for the control volume shown have been studied extensively, especially relative to predicting wall/blockage effects on propellers and wind turbines, as in [1,10–12], among others. In [9], the subject was revisited by applying a momentum, mass, and energy balance to the flow structure and the cuts of Fig. 1. The following assumptions were applied:

1) Inviscid incompressible flow is through a conduit of constant cross-sectional area A_c.

2) Flow with uniform pressure and velocity enters at upstream infinity.

3) Flow exits at downstream infinity at uniform pressure p_o with a slipstream between the mainstream fluid exiting at velocity V_c and the fluid exiting at velocity V_o, which passed through the rotor/disk.

4) The cuts around the rotor/disk shrink to its surface.

5) The thrust on the rotor/disk equals the pressure jump acting on the area A_p:

$$\text{Thrust} = A_p(p_1 - p_2) \tag{1}$$

As shown in [9], the mass, momentum, and energy equations can be reduced to the form

$$C_D(u_c + u_o) = (u_c - u_o)\left[1 + \frac{u_c - 1}{2u_o}\right]^2 \tag{2}$$

$$(u_c - 1)(2u_o + u_c - 1) = \alpha(u_c^2 - u_o^2) \tag{3}$$

where the nondimensional velocities are defined as

$$u_o \equiv V_o/V_a, \qquad u_c \equiv V_c/V_a \tag{4}$$

the disk loss coefficient is defined as

$$C_D \equiv \frac{1}{4}\frac{(p_1 - p_2)}{\frac{1}{2}\rho V_p^2} \tag{5}$$

Received 18 February 2009; revision received 21 August 2010; accepted for publication 8 October 2010.

*Founder and Senior Technical Advisor, 380 Main Street. Fellow AIAA.

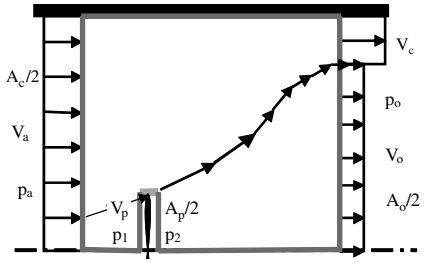

Fig. 1 Control volume.

and the flow-domain/conduit area or blockage ratio is defined as

$$\alpha \equiv A_p/A_c \tag{6}$$

Equations (2) and (3) are a compact form of those presented by Mikkelsen and Sørensen [10] and have the advantage that they directly reduce to the classic wind turbine equations when $\alpha = 0$.

Three additional flow parameters of interest are the rotor/disk velocity ratio,

$$u_p \equiv \frac{V_p}{V_a} = u_o \frac{u_o + u_c}{2u_o + u_c - 1} \tag{7}$$

the rotor/disk thrust coefficient,

$$C_T \equiv \frac{(p_1 - p_2)}{\frac{1}{2}\rho V_a^2} = u_c^2 - u_o^2 \tag{8}$$

and the power coefficient:

$$C_P \equiv \frac{(p_1 - p_2)A_p V_p}{\frac{1}{2}\rho A_p V_a^3} = \frac{u_o(u_c + u_o)^2(u_c - u_o)}{2u_o + u_c - 1}$$
$$= u_p(u_c^2 - u_o^2) = u_p C_T \tag{9}$$

Mikkelsen and Sørensen [10] provided numerical solutions for blockage levels up to 25% and induction factors up to 0.6 using a different form of the same governing equations. In [9], the current author expanded the results of [10] using Eqs. (2) and (3) for the same blockage range, but was able to extend the results to the stall condition, i.e., to an induction factor of 1. Figures 2 and 3 add to those of [9] by presenting solutions to Eqs. (2) and (3) for values of α very near zero. Figure 2a shows the traditional power-coefficient versus thrust-coefficient curves for blockages from 0.1 to 2%, and Fig. 2b expands this for the range of 0.01 to 0.1%. Figure 3 provides a broader set of results in terms of the disk loading coefficient C_D, which was found in [9] to be provide more insight into the physics of the problem. Also shown throughout Figs. 2 and 3 are familiar solutions to the equations for zero blockage ($\alpha = 0$), for which Eqs. (2) and (3) can be solved in closed form to give the classical solution:

$$u_c = 1, \qquad u_O = \frac{1 - C_D}{1 + C_D} \tag{10}$$

$$C_P = 4\frac{C_D}{(1 + C_D)^3} = \frac{1}{2}C_T[1 + \sqrt{1 - C_T}] \tag{11}$$

$$u_p = \frac{1}{(1 + C_D)} \tag{12}$$

For this limit solution at $\alpha = 0$, as shown in Figs. 2a, 2b, and 3a, C_P abruptly stops at a value of 0.5 when $C_D = C_T = 1$, because as indicated in Fig. 3b, $u_o = 0$ at this point and Eq. (10) indicates that u_o would be less than zero thereafter, which is not allowed. However, the results for small blockage levels presented in Figs. 2 and 3 imply a possible different outcome. First, consider the results in Fig. 3. Figures 3a and 3c show that well-behaved steady-state solutions exist, as all cases with nonzero blockage pass smoothly through the singularity point, $C_D = 1$, even for blockage as low as 0.1%. However, Fig. 3b indicates a possible complication. Although the solution curves are continuous and smooth for all cases with nonzero blockage, they also clearly imply that a discontinuous change in the slope will occur at $C_D = 1$ for the limit case of zero blockage. The latter result is the root cause of the issue addressed here. It clearly indicates that in the limit of zero blockage for $C_D > 1$, C_P and u_p are well-behaved, while $u_O = 0$ for all these cases. Or, seen another way, C_D is apparently not unique for $u_O = 0$. The latter point is also manifest in Fig. 2b, where it is shown that as one approaches the zero-blockage condition, at $C_T = 1$ there are apparently an infinity of values for C_P. The remaining issue is to determine the relationships that represent the implied solutions at the limit of zero blockage for $C_D > 1$.

Resolution of this issue starts with the recognition, from Fig. 3b, that for $C_D < 1$, $u_o > 0$ for all values of α, including zero. Thus, the limit forms of the governing equations, as given in Eqs. (10–12), are straightforwardly recovered from Eqs. (2) and (3) for $C_D < 1$ by setting $\alpha = 0$ in Eq. (3) to give $u_c = 1$, thereby eliminating the last term in Eq. (2). However, for all $C_D > 1$, Fig. 3b shows that, for a fixed value of C_D, u_o approaches zero as α decreases toward zero. The latter result renders the last term in Eq. (2) indeterminate for $C_D > 1$, as α becomes vanishingly small and u_c necessarily approaches 1. Thus, in the region of $C_D > 1$, a limit analysis is required to determine the applicable form of Eqs. (2) and (3) for vanishingly small α. Following standard perturbation principles, the analysis starts by introducing a small parameter ε, such that in an inner region near $u_o = 0$, the velocity components can be written to lead order as

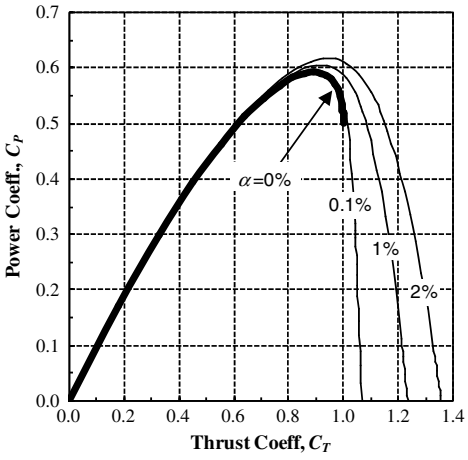

a) Full spectrum

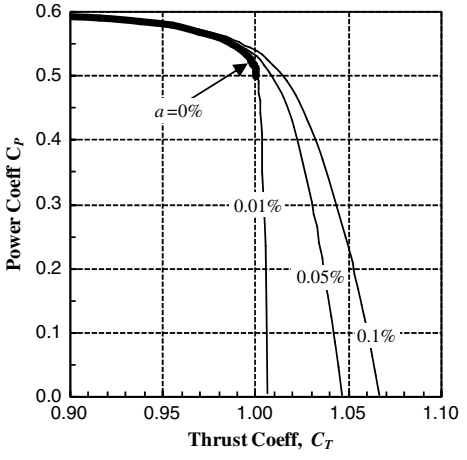

b) Expanded scale

Fig. 2 Thrust singularity.

$$u_o = \varepsilon U_o, \qquad u_c = 1 + \varepsilon U_c \tag{13a}$$

which, when introduced in Eq. (3), leads to the conclusion that

$$\varepsilon = \sqrt{\alpha} \tag{13b}$$

and

$$U_o = \frac{1}{2}\frac{1 - U_c^2}{U_c} \tag{13c}$$

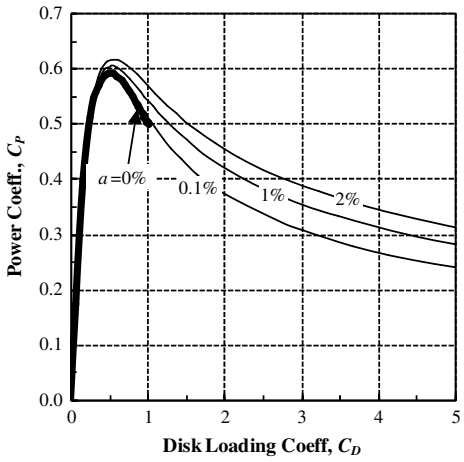

a) Power

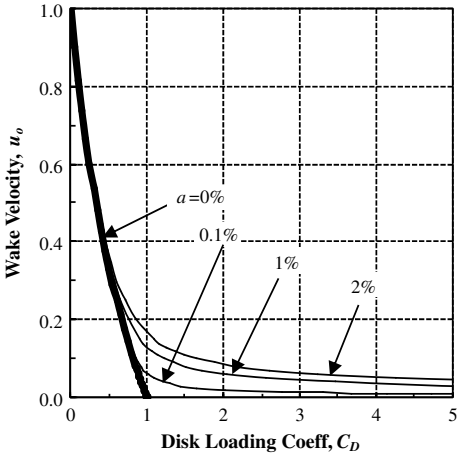

b) Wake velocity

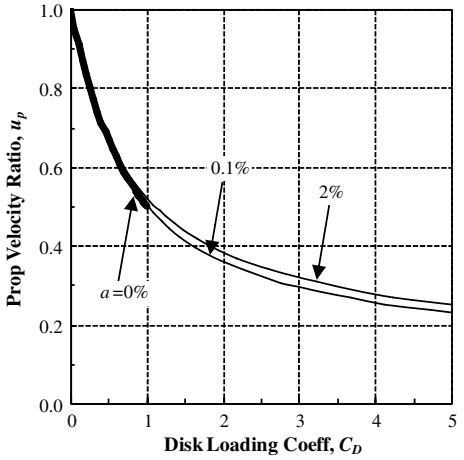

c) Prop velocity

Fig. 3 Disk-loss-coefficient dependency.

These results are then used in Eq. (2) to solve for U_c and thus provide relations for u_o and u_c for any vanishingly small value of α when $C_D > 1$. Using the resulting expressions in Eqs. (7–9) one arrives at the following relations that are valid for all $C_D > 1$ in the limit of zero blockage,

$$u_O = \mathcal{O}(\sqrt{\alpha}) \tag{14a}$$

$$u_c = 1 + \mathcal{O}(\sqrt{\alpha}) \tag{14b}$$

$$C_T = 1 + \mathcal{O}(\sqrt{\alpha}) \tag{14c}$$

and to first order:

$$C_P = u_p = \frac{1}{2\sqrt{C_D}} \tag{14d}$$

The resulting new solutions for $\alpha = 0$ are shown in Figs. 4a–4c, where the classical solution given by Eqs. (10–12) is applied for C_D up to unity, and the new solution, represented by Eqs. (14a–14d), applies for C_D greater than unity. Glauert's empirical expression is also shown for later discussion.

III. Discussion of Results

Several pertinent observations can be made relative to the analysis above and the results provided in Figs. 2–4.

1) First, it is important to keep in mind that the results provided in Eqs. (14a–14d) are exact solutions of the control-volume actuator-disk model of the steady-state conservation laws as given in Eqs. (2) and (3) for the particular situation depicted in Fig. 1. All the flow entering on the left exits on the right at either velocity u_c outside the wake or $u_o = 0$ inside the rotor/disk wake. In passing, it is also worthy of note that the only one-dimensional aspect of the model is that it assumes that the velocity at the rotor/disk does not vary across its area.

2) These new solutions apply for any cross-sectional area conduit in the limit as that conduit's area becomes infinity large compared with the disk/rotor area. As such, they provide a rational pathway to the zero-blockage solution of the conservation laws for flow through or around a disk. They resulting solution family given in Eqs. (14a–14d) only exists for $C_D > 1$ and cannot be recovered from the governing equations at the limit of zero blockage, i.e., Eqs. (10–12). They can only be recovered from the more general form given in Eqs. (2) and (3) for blockage levels approaching zero.

3) The new solution family for zero blockage is shown in Fig. 4 to be the natural extension of the finite blockage-solution family, all of which provide a smooth and continuous approach past the maximum power level all the way to the disk stall condition, i.e., $u_p = 0$ and $a = 1$. Thus, the expressions given in Eqs. (14a–14d) provide the heretofore missing piece for the back side of the power curve, bridging the gap between $u_p = 0.5$ ($a = 0.5$) and disk stall, $u_p = 0$ ($a = 1$).

4) This solution family displays a nonunique dependence on the C_T and u_o that can be easily avoided by employing either C_D, u_p, or a as the independent variable.

5) As shown in Fig. 4, the blockage-solution family provides analytically exact alternatives to Glauert's empirically based expression for porous disks. However, it requires careful analysis for application to rotors, as discussed further below.

First, consider the case of flow through or around a porous disk, for which the actuator-disk model has long been applied. Hoerner [13] discussed this case in some detail because of its relevance to numerous important applications, including flow through grills, radiators, parachutes, and more. While providing a summary of data from numerous sources, Hoerner also made three important observations on the topic relevant to current interests:

1) Flow through porous disks approaches flow past a solid disk as the porosity decreases.

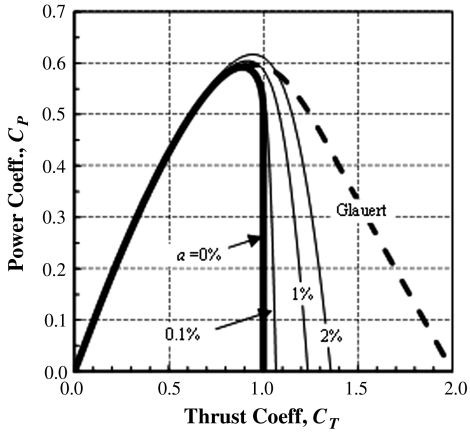

a) Power

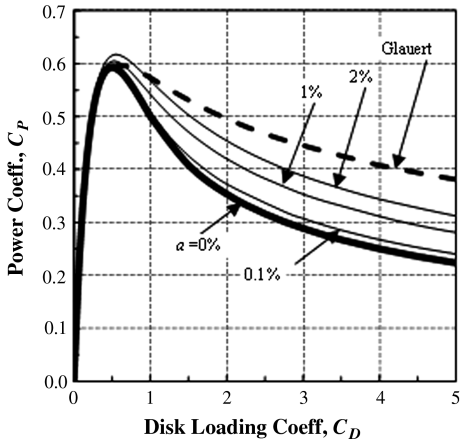

b) Power

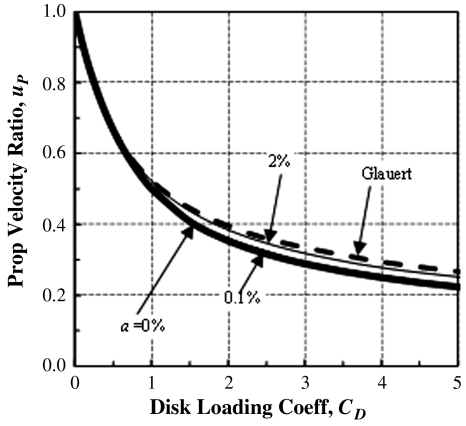

c) Prop velocity

Fig. 4 Limit solution.

2) For Reynolds numbers (based on disk diameter) greater than 300, the flow over a solid disk changed its vortex shedding pattern, and by 1000, the axial force became practically a constant. This observation was reinforced by the experimental results of Knight [14] and Morel and Bohn [15], where no shedding was observed above 100,000. Hoerner [13] further stated that, "Because of this stability, the disk is sometimes employed in the calibration of air streams."

3) Hoerner [13] acknowledged that virtually all the data available to him were influenced, to an undetermined degree, by both by wind-tunnel blockage and freestream turbulence effects.

With these points in mind, the current actuator predictions are compared in Fig. 5 with the experimental data for disks given in [13–15], along with Glauert's empirical expression. The predictions are shown for blockages levels of 0%, as well as 0.44 and 1.1%, corresponding to the test conditions of [14,15], respectively. From both Figs. 5a and 5b, it seems clear that the current predictions better represent the data than does Glauert's expression, thereby indicating that high-Reynolds-number flow past disks does not enter a turbulent-wake state.

Figure 6 further addresses this point using the CFD studies of [6,7]. Both of those studies were conducted with a blockage level of 1% and are seen to follow the current predictions as well as Glauert's expression. Mikkelsen [7] repeated Sørensen et al. 's [6] case for $C_T = 1$, but with the computational domain extended downstream 20 radii, as compared with 10 radii [6], and the Reynolds number increased from 1000 to 5000. It is shown in Fig. 6 that the current predictions virtually reproduce Mikkelsen's [7] CFD results for all induction levels. Mikkelsen also stated that a $C_T = 1$ was achieved at $a = 0.42$, as compared with the reported value of 0.39 [7] and the classical theory level of 0.5. The current solutions predict $C_T = 1$ at $a = 0.42$ for 1% blockage, in precise agreement with Mikkelsen's results. For $C_T = 1.1$ Sørensen et al.'s [6] result lies between the current predictions and Glauert's expression, while for $C_T > 1.1$ they reported significant numerical convergence problems and solutions with reverse flow ahead of the rotor/disk. While it is tempting to assume the latter behavior is associated with entry into the turbulent-wake state, it is also possible that it is associated with the low Reynolds number of 1000 used in [6]. Per the above discussion, it seems reasonable to assume that higher-Reynolds-number cases would be numerically stable. In a limited-scope study with a Reynolds numbers of 10^7 by the author using the CFX CFD code, no difficulty was encountered recovering CFD solutions up to, and including, $C_T = 1.2$ with blockage levels from 0.02 to 1%. Some of these solutions did contain a recirculating bubble of fluid aft of the disk, because some of the streamlines that passed through the disk did not have enough total pressure to sustain the diffusion levels

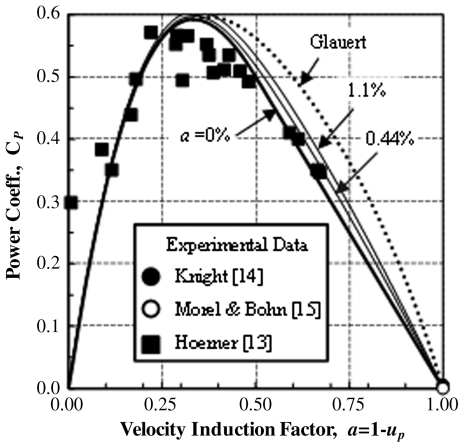

a) Power

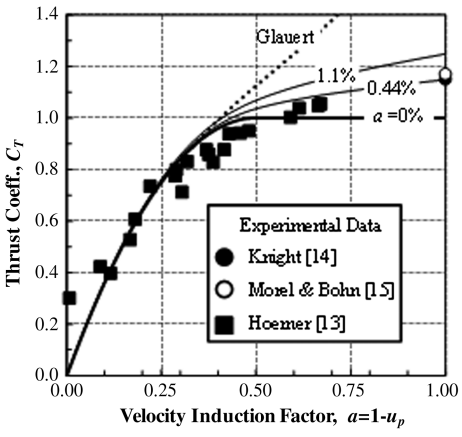

b) Thrust

Fig. 5 Experimental actuator-disk comparisons.

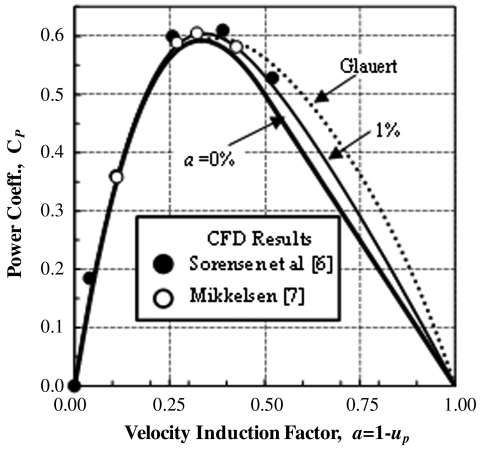

a) Power

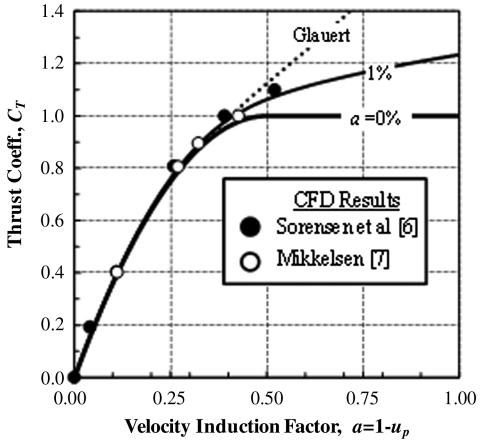

b) Thrust

Fig. 6 CFD actuator-disk comparisons.

required. However, these bubbles were quickly closed down by the turbulent shear layer mixing and proceeded smoothly into a classical far-wake mixing spread. It is reasonable to anticipate that CFD methods that impose a C_T higher than allowed by the current model might well encounter numerical instabilities that could be mistaken as a manifestation of a turbulent-wake state.

IV. Conclusions

Based on a rigorous limit analysis of the control-volume/actuator-disk model, new, simple, exact algebraic relations are provided for regions beyond the classic model's singularity at a thrust coefficient of one where the nondimensional rotor velocity decreases from 0.5 to 0. Both experimental and CFD results verify the new model's applicability and utility for high-Reynolds-number flow past disks and reinforce the conclusion that blockage effects must be accounted for, even for levels less than 1%.

There remains the issue of how the actuator-disk results relate to flow through a rotor in the same parameter space. It would seem reasonable to assume that as long as the maximum thrust levels are on the order of the limit values predicted here for the relevant blockage levels, one should anticipate a structured wake state, not a turbulent-wake state. For these cases, though, instabilities might appear due to the presence of swirl and tip vortices in the wake. For thrust levels beyond the predicted maximum levels, either numerical or real instabilities will likely be encountered.

References

[1] Glauert, H., *The Elements of Airfoil and Airscrew Theory*, 2nd ed., Cambridge Univ. Press, Cambridge, England, U.K., 1947.

[2] Wilson, R. E., and Lissaman, P. B. S., *Applied Aerodynamics of Wind Power Machines*, Oregon State Univ., Corvallis, OR, 1974.

[3] Hansen, M. O. L., *Aerodynamics of Wind Turbines*, Cromwell Press, London, 2000.

[4] Gashe, R., and Twele, J., *Wind Power plants*, Solarpraxis, Berlin, 2002.

[5] Stoddard, F. S., "Momentum Theory and Flow States for Windmills," *Wind Technology Journal*, Vol. 1, 1977, pp. 3–9.

[6] Sørensen, J. N., Shen, W. Z., and Munduate, X., "Analysis of Wake States by a Full-Field Actuator Disc Model," *Wind Energy*, Vol. 1, 1998, pp. 73–88. doi:10.1002/(SICI)1099-1824(199812)1:2<73::AID-WE12>3.0.CO;2-L

[7] Mikkelsen, R., "Actuator Disk Methods Applied to Wind Turbines," Ph.D. Dissertation, Fluid Mechanics, Dept. of Mechanical Engineering, Technical Univ. of Denmark, MEK-FM-PHD 2003-02, Lyngby, Denmark, June 2003.

[8] Buhl, M. L., "A New Empirical Relationship Between Thrust Coefficient and Induction Factor for Turbulent Windmill State," National Renewable Energy Lab., Rept. NREL/TP-500-36834, Washington, D.C., Aug. 2005.

[9] Werle, M. J., "Wind Turbine Wall Blockage Performance Corrections," *Journal of Propulsion and Power*, Vol. 26, No. 6, Nov.–Dec. 2010, pp. 1317–1321. doi:10.2514/1.44602

[10] Mikkelsen, R., and Sørensen, J. N., "Modeling of Wind Tunnel Blockage," *Proceedings of the 2002 Global Windpower Conference and Exhibit*, Paris, 2002.

[11] Sørensen, J, Norkaer, S, Wen, Z., and Mikkelsen, R., "Wall Correction Model foe Wind Tunnels with Open Test Section," *AIAA Journal*, Vol. 44, No. 8, Aug. 2006, pp. 1890–1894. doi:10.2514/1.15656

[12] Fitzgerald, R. E., "Wind Tunnel Blockage Corrections for Propellers," M.S. Thesis, Univ. of Maryland, Dept. of Aerospace Engineering, College Park, MD, 2007.

[13] Hoerner, S, F., *Fluid-Dynamic Drag*, Hoerner, Midland Park, NJ, 1965.

[14] Knight, M., "Wind Tunnel Standardization Disk Drag," NACA TN 253, Dec. 1926.

[15] Morel, T., and Bohn, M., "Flow over Two Circular Disks in Tandem," *Journal of Fluids Engineering*, Vol. 102, March 1980, pp. 104–111. doi:10.1115/1.3240599

A. Prasad
Associate Editor